EUROPEAN FUSION DEVELOPMENT AGREEMENT

EFDA–JET–PR(04)70

M.J. Mantsinen, V. Kiptily, M. Laxåback, A. Salmi, Yu. Baranov, R. Barnsley, P. Beaumont, S. Conroy, P. de Vries, C. Giroud, C. Gowers, T. Hellsten, L.C. Ingesson, T. Johnson, H. Leggate, M.-L. Mayoral, I. Monakhov, J.-M. Noterdaeme, S. Podda, S. Sharapov, A.A. Tuccillo, D. Van Eester and EFDA JET contributors

Fast Ion Distributions Driven by Polychromatic ICRF Waves on JET

Fast Ion Distributions Driven by Polychromatic ICRF Waves on JET

M.J. Mantsinen[1], V. Kiptily[2], M. Laxåback[3], A. Salmi[1], Yu. Baranov[2], R. Barnsley[2], P. Beaumont[2], S. Conroy[3], P. de Vries[2], C. Giroud[4], C. Gowers[2], T. Hellsten[3], L.C. Ingesson[4,5], T. Johnson[3], H. Leggate[2], M.-L. Mayoral[2], I. Monakhov[2], J.-M. Noterdaeme[6,7], S. Podda[8], S. Sharapov[2], A.A. Tuccillo[8], D. Van Eester[9] and EFDA JET contributors*

[1]Helsinki University of Technology, Association Euratom-Tekes, Finland
[2]Association Euratom-UKAEA, Culham Science Centre, Abingdon OX14 3DB, UK
[3]Euratom-VR Association, Stockholm, Sweden
[4]FOM-Rijnhuizen, Association Euratom-FOM, TEC, Nieuwegein, NL
[5]EFDA CSU-Garching, Garching, Germany
[6]Max-Planck IPP-EURATOM Assoziation, Garching, Germany
[7]Gent University, EESA Department, Belgium
[8]Associazione EURATOM-ENEA sulla Fusione, CR Frascati, Frascati, Rome, Italy
[9]LPP-ERM/KMS, Association Euratom-Belgian State, TEC, Brussels, Belgium
See appendix of J. Pamela et al., "Overview of JET results", in Proc of 19th IAEA Fusion EnergyConference, Lyon, 2002 (IAEA, Vienna, 2003) Partner in the Trilateral Euregio Cluster (TEC)*

Preprint of Paper to be submitted for publication in
Plasma Physics and Controlled Fusion

ABSTRACT

Experiments have been carried out on the JET tokamak to investigate fast ^{3}He and hydrogen minority ion populations accelerated by ICRF waves launched with multiple frequencies (i.e. up to four frequencies separated by up to ≈ 15%). This "polychromatic" heating is compared to single-frequency, "monochromatic", ICRF heating of reference discharges with similar power levels. Information on the fast ion populations is provided by two-dimensional gamma-ray emission tomography and the measurements are compared with numerical modelling. Polychromatic heating with resonances in the plasma centre ($R_{res} \approx R_0$) and on the low magnetic-field side ($R_{res}>R_0$) is found to produce predominantly high-energy standard trapped ions, while resonances on the high magnetic-field side ($R_{res}<R_0$) increase the fraction of high-energy passing ions. Monochromatic heating with a central resonance produces stronger gamma-ray emission with the maximum emission in the midplane close to, and on the low magnetic-field side of, the resonance, in agreement with the calculated radial distribution of fast ion orbits. Both the fast ion tail temperature and energy content are found to be lower with polychromatic waves. Polychromatic ICRF heating has the advantage of producing smaller-amplitude and shorter-period sawteeth, consistent with a lower fast ion pressure inside the q = 1 surface, and higher ion to electron temperature ratios.

1. INTRODUCTION

During heating with waves in the ion cyclotron range of frequencies (ICRF), the distribution function of the resonating ions is driven towards a non-Maxwellian state with an anisotropic high-energy tail developing mainly in the perpendicular velocity direction [1]. The fast ions play an important role for the resulting plasma heating and affect the stability properties of the plasma. For example, the energy distribution of the fast ions determines the electron versus ion heating fraction. Furthermore, the fast ions affect plasma instabilities such as sawteeth and fishbone modes, and contribute to the plasma pressure which is often bounded by stability limits. Therefore, it is important to have a number of ways to modify the ICRF-driven fast ion distribution function. The most commonly used techniques include varying the resonance position and resonant ion density, as well as inducing radial transport of the resonant ions with toroidally directed waves [2-5]. In this paper we investigate possibilities to influence fast ICRF-driven populations using multi-frequency (polychromatic) heating, as opposed to the more common single-frequency (monochromatic) heating. Due to its lower average power density and thereby lower average energy of fast ions, polychromatic heating has potential for the key task of controlling and optimising the ion heating profile in present-day and future tokamak plasmas, with the radial spread being controlled by the frequency shifts of the different ICRF antennas.

Hydrogen minority ICRF heating with multiple frequencies was routinely used in high-performance NBI-dominated plasmas on the JET tokamak before and during the 1997 deuterium-tritium campaign [6]. Using up to four ICRF frequencies, the ion cyclotron resonances were spread over a 30-40cm wide region in the plasma centre in order to decrease the power density and thereby

improve bulk ion heating and plasma stability. However, no direct one-to-one comparisons between monochromatic and polychromatic ICRF heating were obtained at that time. ICRF waves with multiple frequencies have also been applied in plasmas with internal transport barriers in Alcator C-mod[7] and in fast wave current drive experiments on DIII-D [8, 9]. Recently , code simulations that have been carried out to predict the performance of monochromatic and polychromatic ICRF heating in ITER [10] and the JET enhancement project [11] suggest significantly better ion heating and fusion performance with polychromatic heating. Since the physics of polychromatic ICRF heating is rather complex, as we will discuss in Section 2, a more detailed experimental assessment of its effects is of interest.

This paper presents experiments carried out on the JET tokamak using polychromatic ICRF heating of ^{3}He and hydrogen minority ions, including comparisons with single-frequency operation. In particular, polychromatic heating with resonances either on the low magnetic-field side (i.e. with the major radius of the resonance R_{res} larger than the major radius R_0 of the magnetic axis) or high magnetic-field side ($R_{res}<R_0$) of the tokamak are compared with central monochromatic heating ($R_{res} \approx R_0$) for a number of different ICRF powers. Special emphasis is on the detailed measurements of ICRF-driven ion distribution functions, in particular their radial profile, using gamma-ray emission tomography [12, 13] and in the comparisons with ICRF modelling taking into account the physics of polychromatic heating. While the primary interest in polychromatic ICRF heating comes from the higher bulk plasma ion to electron heating ratio expected with the lower power density, the present gamma-ray emission tomography measurements are sensitive mainly to high-energy ions heating predominantly bulk electrons. Consequently, no optimisation of the bulk ion heating has been attempted and the present paper can be viewed as one of the first steps only in exploring the physics of polychromatic ICRF heating.

The paper is organised as follows. The physics of polychromatic ICRF heating is discussed in Section 2, followed by an overview of the experiments in Section 3. The results of the experiments and their analysis are presented in Section 4. Finally, Section 5 gives the conclusions.

2. PHYSICS OF POLYCHROMATIC ICRF HEATING

By dividing power between different frequencies and thereby between different cyclotron resonance layers separated in tokamak major radius, polychromatic ICRF heating decreases the flux-surface-averaged power density p_{ICRF} as compared with central single-frequency heating. The lower p_{ICRF} is important in many respects. Firstly, it results in a lower average energy ε_{fast} of the ions in the high-energy tail of the resonant ion distribution function, according to the scaling $\varepsilon_{fast} \approx p_{ICRF}\tau_s /2n_{fast}$, where τ_s and n_{fast} are the fast ion slowing down time and density, respectively. Subsequently, a higher ion-to-electron heating ratio is expected as these ions transfer the ICRF heating power to the bulk plasma through Coulomb collisions. The lower power density plays also an important role for the details of the fast ion distribution. At low power densities for which the resonant ions have energies below the critical energy [1] $E_{crit} = 23.5T_eA^{1/3} (\Sigma_j n_j Z_{2j} / n_e)^{2/3}$, where A is the atomic mass of the

resonant ions and the electron temperature T_e is in eV, pitch-angle scattering is strong and the orbits of the resonant ions frequently change between trapped and passing. As a result, a rather isotropic fast ion energy distribution can be expected. At higher power densities, the resonant ions reach energies above the critical energy and experience weaker scattering in pitch-angle. As a result, the fraction of trapped ions increases, and the distribution function of the resonant ions is driven towards a non-Maxwellian state with an anisotropic high-energy tail developing mainly in the perpendicular velocity direction.

The detailed physics of polychromatic ICRF heating can be studied with a three-dimensional orbit-averaged Fokker-Planck equation [14]

$$\frac{\partial f}{\partial t} = \langle C(f) \rangle + \langle Q(f) \rangle \tag{1}$$

where <...> denotes averaging over unperturbed orbits, C is the collision operator describing collisions with background ions and electrons and Q is a quasi-linear operator describing wave-particle interactions. The distribution function is a function of three invariants of the unperturbed particle motion as well as an orbit label σ to distinguish different orbits corresponding to the same triplet of invariants, e.g. co- and counter current passing orbits [15].

By choosing the invariants of unperturbed particle motion to be energy E, $\Lambda=\mu B_0/E$ and toroidal angular momentum P_φ, where μ is the magnetic moment and B_0 is the on-axis magnetic field, the quasi-linear operator can be written as [16]

$$\langle Q(f) \rangle = \Sigma \; L_N \left(D_{RF}^N \, L_N \, f \right) \tag{2}$$

where

$$L_N = \omega \; \frac{\partial}{\partial E} \; + \; \frac{n\omega_{c0} - \Lambda\omega}{\partial \Lambda} \; \frac{\partial}{\partial \Lambda} \; + N \; \frac{\partial}{\partial P_\varphi} \; , \tag{3}$$

is the diffusion coefficient resulting from the interaction with the wave component with the toroidal mode number N at an ion cyclotron resonanc*e* , where is the cyclotron harmonic.

From the characteristics of the operator in Eq. (3) we find that the changes in and in the toroidal angular momentum P_j due to wave-particle interactions are linked to the change in energy E as

$$\Delta\Lambda = \frac{n\omega_{c0} - \Lambda\omega}{\omega E} \; \Delta E$$

and

$$\Delta P_\varphi = \frac{N}{\omega} \; \Delta E \, .$$

These equations describe the characteristics in phase space for ions interacting with a wave with a given mode number and frequency. In particular, we can see that an increase in the ion energy due

to interaction with the wave drives Λ towards $\Lambda_{res} = n\omega_{c0} / \omega$; i.e. the turning points of the trapped ion orbits are driven towards the unshifted cyclotron resonance $\omega = n\omega_{ci}$. Also, we can see that for monochromatic ICRF heating with a single frequency, interactions with waves with a fixed toroidal mode number *N* gives rise to one-dimensional diffusion in phase space. However, for a spectrum of toroidal mode numbers, diffusion becomes two-dimensional because a resonant ion may approach $\Lambda_{res} = n\omega_{c0} / \omega$ along different characteristics corresponding to different *N*. Polychromatic ICRF heating adds a third dimension to the diffusion process since an ion may be in resonance with several frequencies, each with a different $\Lambda_{res} = n\omega_{c0} / \omega$.

The total change in Λ during an orbit depends on several quantities. Firstly, it depends on the amount of power applied at the frequencies with which the ion is in resonance. Secondly, it depends on the spatial separation of these resonances. Thirdly, it depends on the toroidal mode number spectrum of the wave through the effects of different Doppler shift $\omega = n\omega_{ci} + k_{||}v_{||}$ where $k_{||}$ and $v_{||}$ are the parallel wave number and parallel velocity of the ion, respectively. Since the trapped ion orbit extends to the low magnetic-field side of its turning points, a significant Doppler shift is typically required for the ion to be in resonance with waves for which the unshifted cyclotron resonances $\omega = n\omega_{ci}$ is on the high magnetic-field side of the orbit turning points. Thus, one could expect the dominant Λ-drift of trapped ions to be towards the lower-frequency resonances. However, for ion energies below the critical energy E_{crit}, strong pitch-angle scattering tends to restore the Λ-spectrum. As discussed at the beginning of this section, pitch-angle scattering is expected to be stronger for polychromatic ICRF due to the lower average power density and thereby lower average fast ion energy. At high ICRF powers, however, high ion energies can be obtained even with polychromatic ICRF and for trapped orbits the dominant Λ-drift towards lower-frequency resonances may cause the orbits to detach from higher-frequency resonances. This can lead to a drift of the turning points to the lower-frequency resonance (i.e. in the direction of larger major radius) [17]. Finally, we note that the number of high-energy ions with passing orbits increases when a resonance is moved from the centre or the low magnetic-field side (LFS) to the high magnetic-field side (HFS) of the tokamak both in the case of polychromatic and monochromatic heating. This is because in the case of a HFS resonance the ICRF-accelerated ions are closer to the boundary between trapped and passing ions.

In this paper, we use the ICRF codes PION [18] and SELFO [19, 20] to simulate the effects of polychromatic ICRF and to analyse the experimental results. The PION code calculates the pitch-angle-averaged distribution function of the resonant ions with a simplified one-dimensional Fokker-Planck equation for the whole ICRF heating phase. The SELFO code solves Eq.1 for the three-dimensional distribution function of the resonant ions using the Monte-Carlo method and taking into account the effects of finite orbit widths and RF-induced spatial transport. The SELFO analysis is performed for specific time-points during the steady ICRF phase of the discharge, and the code is run until the fast ion energy saturates and the RF power absorbed by the resonant ions equals the collisional heating power.

3. OVERVIEW OF THE EXPERIMENTS

The experiments were carried out in L-mode deuterium plasmas in a single-null divertor configuration at a magnetic field of 3.25–3.7T and a plasma current of 1.8–2MA. ICRF frequencies in the range of 33-38 MHz were used for ^{3}He minority heating, with the total coupled power in the range of 3-4.5MW. Higher power, about 7MW, was obtained using hydrogen minority heating with frequencies in the range of 46-52MHz. For monochromatic heating, the resonance was located in the plasma centre, and the natural spread in the frequencies delivered by the four JET A2 ICRF antennas [21] gave rise to a 5-10cm spread in major radius of the resonances. For polychromatic operation, the resonances were spread in major radius over a larger, typically 30-40cm wide, area in the plasma centre and on the low magnetic-field side (LFS) or high magnetic-field side (HFS). The dipole ($0\pi0\pi$) phasing of the antennas was used with a symmetric toroidal mode number spectrum peaked around $N \approx \pm 26$, the ^{3}He concentration $n(^3\mathrm{He})/n_e$ was about 1%, and the hydrogen concentration n_H/n_e was about 3-4%.

A summary of the discharges is given in Table I, including the radial positions of the cyclotron resonances and the partitioning of power between them. In total, four sets of discharges are analysed, each of which consists of one discharge with monochromatic ICRF heating and one (or two) discharges with polychromatic ICRF heating. Comparisons between the discharge sets also provide a scan in power at similar resonance positions as well as a scan in the resonance positions from the HFS to the LFS at a similar power.

4. RESULTS

4.1 ICRF HEATING WITH MULTIPLE RESONANCES ON THE HFS AS COMPARED WITH A SINGLE CENTRAL RESONANCE

The time traces of the main plasma parameters for Pulse Nos: 56532, 56533 and 56535 with up to 3.5MW of ^{3}He minority heating are shown in Fig.1. For Pulse No: 56532 the fundamental ^{3}He ion cyclotron resonances are located close to the plasma centre, while for Pulse Nos: 56535 and 56533 they are spread over a 30cm wide region from the plasma centre towards the HFS. The difference between Pulse Nos: 56535 and 56533 is the power split between the different frequencies, with more power further off-axis in Pulse No: 56533 (cf. Table I).

As we can see in Fig.1, polychromatic ICRF heating gives rise to a somewhat lower plasma diamagnetic energy and lower central electron temperature as well as to a shorter sawteeth period, suggesting a lower fast ion energy in the plasma centre inside the q = 1 surface. According to the ICRF modelling codes PION and SELFO, the observed differences in the plasma diamagnetic energy are dominantly due to differences in the total fast ion energy, with differences in the plasma thermal energy content playing a smaller role. The fast ion energies W_{fast} as calculated by PION are shown in Fig.2. They are in broad agreement with W_{fast} of 160, 150 and 280kJ for Pulse Nos: 56535, 56533 and 56532, respectively, as given by SELFO at t = 11s. The largest difference in W_{fast} as given by the PION and SELFO codes is for Pulse No: 56533 and is found to be due to stronger direct electron damping predicted by PION for this discharge. The somewhat lower central

electron temperatures with polychromatic heating appear consistent with the broader calculated profiles of total (collisional and direct fast wave) electron heating (Fig. 3). (Mode conversion has been estimated with the Budden formula [22] and found negligible at the low minority ion concentrations of the discharges studied in the present paper.)

Important information on the density distribution of fast ions is obtained with gamma-ray emission tomography [12, 13] (Fig.4). For Pulse Nos: 56532 and 56535, as for the other pulses with ^{3}He minority heating discussed in the present paper, the gamma-ray emission shown in Figs.4(a) and 4(b) is mainly due to nuclear reactions between fast ^{3}He ions with energies above a threshold energy of about 0.9MeV, and ^{9}Be, which is one of the impurity ion species in JET plasmas. Above the threshold energy, the gamma-ray reaction cross-section increases with the fast ion energy. Thus, the gamma-ray emissivity is due to fast ions with very high energies. In particular, the threshold energy for gamma-ray emission is significantly higher than the energy of ≈ 150-200keV above which pitch-angle scattering of ^{3}He ions becomes weak in these pulses. However, as we will show later on in this section, the normalised profiles in major radius of the fast ion distributions within 0.3m from the midplane as calculated with SELFO, taking into account fast ions above a given threshold, do not change very much when the threshold in energy is varied from 0.1 to 0.9MeV. Consequently, the measured gamma-ray emissivity profiles appear to be a rather good representation of the spatial distribution of all fast ions in the pulses presented here. Unless otherwise stated, we have in the following adopted a fixed energy threshold of 0.9MeV when deducing the distributions of fast ions from SELFO simulations.

As we can see in Fig.4(b), the maximum gamma-ray emissivity is shifted slightly to the low magnetic-field side of the central resonances in Pulse No: 56532. For the polychromatic heating in Pulse No: 56535 (Fig.4(a)), the gamma-ray emissivity is more symmetric around the plasma magnetic axis. Emission on the HFS of the magnetic axis with polychromatic ICRF is consistent with a larger number of passing ions with HFS resonances. Indeed, according to the SELFO code, due to the HFS resonances the polychromatic heating in Pulse No: 56535 results in a larger fraction of the high-energy (E > 0.9MeV) ions that have passing orbits encircling the magnetic axis than trapped orbits (about 60 and 30%, respectively). With the monochromatic heating in Pulse No: 56532 the fraction of the high-energy ions that have passing orbits decreases to about 35% and the fraction that have trapped orbits increases to about 55%. The slight shift of the maximum gamma-ray emissivity off-axis on the LFS of the centrally located resonance for Pulse No: 56532 is in agreement with the radial distribution of high-energy ion orbits calculated with the SELFO code. According to SELFO, this shift of the maximum emissivity off-axis is largely due to trapped ions and non-standard passing ions residing entirely on the LFS of the magnetic axis.

For Pulse No: 56533, where more power was applied on the HFS than in Pulse No: 56535, the profile of the gamma-ray emissivity is similar to that for Pulse No: 56535 but the total emission is smaller by a factor of about two. The measured gamma-ray emissivity profiles in the midplane for the three pulses are shown in Fig.5, together with the calculated radial profiles of the fast ion

(E > 0.9MeV) distributions within 0.3m from the midplane. The agreement between the shapes of the simulated radial distributions of fast ions and the experimental gamma-ray emissivity profiles in the midplane is good. These results clearly demonstrate that the radial fast ion profile becomes broader and the number of high-energy ^{3}He ions decreases with a HFS polychromatic scheme when the fraction of power applied off-axis is increased. The broader radial profile of fast ions and the lower W_{fast} for polychromatic ICRF is consistent with the smaller-amplitude and shorter-period sawteeth produced with polychromatic ICRF (c.f. Fig.1).

The fast ion distribution profiles within 0.3m from the midplane have also been calculated with the SELFO code for different thresholds in fast ion energy. Figure 6 shows the resulting normalised profiles of the distribution of fast ions with energies above 0.1, 0.3 and 0.9MeV in Pulse Nos: 56533 and 56532. For Pulse No: 56533 with polychromatic heating, a large fraction of the high-energy ions are in passing orbits. As a result, the normalised calculated fast ion distribution profiles are similar for all energy thresholds, i.e. centred around the magnetic axis and having widths closely determined by the location of the cyclotron resonance that is furthest away from the magnetic axis on the high magnetic-field side. For Pulse No: 56532 with monochromatic heating, the fraction of the ions that are in trapped orbits with the turning points close to the cyclotron resonance increases with energy. As a result, the normalised fast ion density distribution decreases somewhat on the high magnetic-field side of the magnetic axis with increasing energy threshold. Similar results have been obtained for the other discharges presented in this paper. These results indicate that the measured gamma-ray emissivity profiles provide rather good representations of the spatial distributions of fast ions also with energies below the gamma-ray reaction threshold in the present pulses.

4.2 COMPARISON OF ICRF HEATING WITH MULTIPLE RESONANCES ON THE LFS AND HFS

When 3MW of polychromatic heating is applied on the LFS rather than on the HFS as in the discharges presented in Section 4.1, somewhat larger differences in the central electron temperatures are found as compared with a single resonance in the plasma centre. This is revealed by Fig.7 showing the main plasma parameters for two pulses, i.e. reference Pulse No: 57245 with monochromatic heating with the resonance in the plasma centre and Pulse No: 57252 with a spread of about 40cm in the resonances in the plasma centre and on the LFS (c.f. Table 1). Indeed, the central electron temperature is about 20-25% (15%) lower with polychromatic heating with LFS (HFS) resonances than with monochromatic heating with a central resonance. PION and SELFO code modelling suggests that this difference in the electron temperatures for polychromatic heating with LFS and HFS resonances, as compared with monochromatic heating with central resonance, is due to differences in the direct electron heating by the launched fast waves, while different fast ion orbits for LFS and HFS resonances play a smaller role. Fast wave direct electron heating, which is centrally located, increases according to the simulations with the distance between the antenna and the resonance.

It is important to note that while there is a difference between the electron temperature profiles, the ion temperature profiles are similar with polychromatic and monochromatic heating (Fig.8). The calculated bulk electron and ion heating profiles (Fig.9), including the direct fast wave electron heating, appear not to contradict the measured temperature profiles. The power partition between bulk ion and electron heating as given by the PION and SELFO codes are similar, with PION giving a somewhat (15-20%) larger total bulk ion heating.

Gamma-ray emission tomography reveals an increase in the fraction of trapped fast ^{3}He ion orbits when going from the HFS to the LFS polychromatic scheme. This is illustrated by Fig.4(c) for Pulse No: 57252 with LFS resonances and a maximum gamma-ray emissivity on the LFS of the plasma centre, and by Fig.4(a) for Pulse No: 56535 with HFS resonances and a more symmetric gamma-ray emission around the magnetic axis. For the reference Pulse No: 57245 with the same total ICRF power as in Pulse No: 57252 but with monochromatic heating, the gamma-ray emissivity peaks off-axis on the LFS of the centrally located resonance (Fig.4(d)). These results appear to be broadly consistent with the radial distributions of high-energy ions calculated with the SELFO code (Fig.10). According to SELFO, the fractions of different fast ion orbit types above 0.9MeV are similar, i.e. about 70-75% of trapped ions and about 20% of ions with non-standard passing orbits, in Pulse Nos: 57252 and 57245. For the used power distributions among the different resonance layers, the calculated distribution of fast ions with energies above 0.9MeV peaks in the midplane off-axis closer to the plasma centre in the case of monochromatic ICRH, which is consistent with gamma-ray emission tomography. According to SELFO, the contribution from trapped ions to the fast ion density distribution responsible for gamma-ray emissivity dominates and the contribution from the non-standard passing ions is a factor of about two smaller than that from trapped ions. The sensitivity of the simulations to the assumed ^{3}He concentration has also been studied. When the ^{3}He concentration is varied between 0.5 and 2%, the relative number of fast ions above 0.9MeV decreases with increasing concentration while only small changes are found in the orbit topology compositions and the overall shapes of the fast ion density profiles.

According to SELFO and PION simulations, about 50% of the difference in the total plasma diamagnetic energy (Fig.7) is accounted for by a difference in the total fast ion energies, with the rest being due to a reduced thermal plasma energy with polychromatic heating. The time evolution of the fast ion energy as given by the PION code for Pulse No: 57252 and 57245 are shown in Fig.11. SELFO gives somewhat larger fast ion energy W_{fast} of 130 and 210 kJ, respectively, at t = 8.5s. The difference in W_{fast} as given by the two codes for the two pulses is similar, about 80kJ.

4.3 HIGHER POWER ^{3}HE MINORITY HEATING WITH MULTIPLE RESONANCES ON THE LFS

When the power is increased from 3MW to 4.5MW using multiple frequencies with resonances in the plasma centre and on the LFS, gamma-ray emissivity increases and the maximum gamma-ray emission shifts to larger major radii (cf. Figs.4(c) and 4(e) for Pulse Nos: 57252 and 57300,

respectively). The increase in gamma-ray emissivity is due to an increase in the total number and/or the energy of fast ions above the gamma-ray reaction threshold of ≈ 0.9MeV, while the shift in major radius of the maximum gamma-ray emissivity is due to an increase in the energy of the fast ions, and thereby broader drift orbits, and the partial detachment of trapped ion orbits from higher frequencies resonances as discussed in Sec.2. According to SELFO, the 1.5MW difference in total power between Pulse Nos: 57252 and 57300 does not significantly change the relative fractions of different fast ion orbit types.

With 4.5MW of monochromatic heating in Pulse No: 57301, the maximum gamma-ray emission in the midplane is located on the LFS of the resonance, but closer to the centrally located resonance than in Pulse No: 57300 with polychromatic ICRF heating (cf. Figs.4(e) and 4(f)). This is similar to the gamma-ray emission measurements for Pulse Nos: 57252 and 57245 with lower power as discussed in Sec.4.2. The analysis of the measured gamma-ray energy spectra with the GAMMOD code [12] gives a ^{3}He ion tail temperature of about 220 ± 50keV for Pulse Nos: 57300 and 57301, with a somewhat lower tail temperature for Pulse No: 57300 with polychromatic ICRF.

4.4 HIGH POWER HYDROGEN MINORITY HEATING WITH MULTIPLE RESONANCES ON THE LFS

Gamma-ray emission tomography for Pulse Nos: 57296 and 57298 with higher-power (7MW) hydrogen minority heating (Figs.4(g)-(h)) adhere to the trends observed in discharges with ^{3}He minority heating with central and LFS resonances (Figs 4(c)-(f)). For Pulse Nos: 57296 and 57298 the gamma-ray emission is mainly from reactions between fast protons and thermal deuterons, requiring fast protons with energies in excess of about 50keV. There is also a contribution from reactions between protons and ^{9}Be, requiring protons at higher energies (E > 0.3-0.5MeV).

It is interesting to note that for pulses with hydrogen minority heating, the neutron yield is significantly higher in the case of monochromatic heating in Pulse No: 57298 (Fig.12). According to simulations with the PION and SELFO codes, with the higher local power density with monochromatic heating, a larger high-energy tail develops on the distribution function of the background deuterium ions that are resonant with the waves at their second harmonic resonance. The enhanced neutron yield results from fusion reactions between ICRF-accelerated and bulk deuterons. The neutron yield reaches a maximum at $t \approx 7.5$s and then starts to decrease. This takes place soon after the appearance of sawteeth at $t \approx 7$s as the on-axis safety factor decreases below one, which suggests that the fast RF-accelerated deuterons are influenced by sawteeth. The presence of fast deuterons in Pulse No: 57298 is confirmed by the measured gamma-ray energy spectra, which show a peak due to reactions between fast deuterons with energies in excess of 0.9MeV and ^{12}C which one of the main impurity ion species in JET plasmas. The fraction of total ICRF power absorbed by deuterons is, however, rather small. According to SELFO and PION modelling, a deuteron damping below 15% of the total ICRF power is enough to fully explain the measured neutron yield.

Finally, we note that line-integrated fast proton distribution functions deduced from a

high-energy neutral particle analyser [23] for Pulse Nos: 57296 and 57298 indicate fast proton tail temperatures that are about 25% higher with monochromatic than polychromatic heating [24], which is broadly consistent with the gamma-ray measurements presented in this paper. Additional, indirect, confirmation of broader fast ion profiles with polychromatic heating is provided by the observations of reduced mode activity in the Alfvén frequency range [24].

CONCLUSIONS

Experiments have been carried out on the JET tokamak to compare monochromatic and polychromatic ICRF heating of ^{3}He and hydrogen minority ions. In general, the experimental results show trends expected from theory. In particular, the fast ion tail temperature and energy content are found to be lower with polychromatic ICRF waves, as expected due to the lower power density. Furthermore, polychromatic heating with resonances in the centre of the plasma and on the low magnetic-field side is found to produce high-energy ions in predominantly standard trapped orbits, while resonances on the high magnetic-field side increase the fraction of high-energy ions that are in passing orbits encircling the magnetic axis. Monochromatic heating with a central resonance produces stronger gamma-ray emission in the midplane close to, and on the low magnetic-field side of, the resonance, consistent with the calculated fast ion radial distributions. The observed higher ion to electron temperature ratios and shorter-period sawteeth make polychromatic ICRF heating promising for further applications.

REFERENCES

[1]. T.H. Stix, *Waves in Plasmas* (American Institute of Physics, New York, 1992).

[2]. L.G. Eriksson, *et al.*, Phys. Rev. Lett. 81 (1998) 1231.

[3]. M.J. Mantsinen, *et al*., Nucl. Fusion 40 (2000) 1773.

[4]. M.J. Mantsinen, *et al*., Phys. Rev. Lett. **89** (2002) 115004:1-4.

[5]. K.H. Finken, *et al*., Phys. Rev. Lett. 73 (1994) 436.

[6]. F.G. Rimini, *et al*., Nucl. Fusion **39** (1999) 1591.

[7]. J.E. Rice, *et al.*, Nucl. Fusion **42** (2002) 510.

[8]. C.C. Petty, *et al*., Nucl. Fusion **39** (1999) 1369.

[9]. C.C. Petty, *et al*., Nucl. Fusion **35** (1995) 773.

[10]. V. Bergeaud, L.G. Eriksson, and D.F.H. Start, Nucl. Fusion 40 (2000) 35.

[11]. M.J. Mantsinen, M.D. Kihlman, and L.-G. Eriksson, 29th European Physical Society Conference on Plasma Physics and Controlled Fusion, 17-21 June 2002, Montreux, Switzerland, Europhysics Conference Abstracts Vol. 26 B, P-1.033 (2002).

[12]. V.G. Kiptily, *et al*., Nucl. Fusion **42** (2002) 999.

[13]. V.G. Kiptily, *et al.*, 'Gamma-Ray Imaging of D and ^{4}He Ions Accelerated by Ion-Cyclotron-Resonance Heating in JET Plasmas,' submitted to Nucl. Fusion Lett.

[14]. L.-G. Eriksson, and P. Helander, Phys. Plasmas **1** (1994) 308.

[15]. J.A. Rome, and Y.-K.M. Peng, Nucl, Fusion **19** (1979) 1193.
[16]. L.-G. Eriksson, M.J. Mantsinen, T. Hellsten, and J. Carlsson Phys. Plasmas **6** (1999) 513.
[17]. M. Laxåback, T. Johnson, T. Hellsten, and M. Mantsinen, 'Self-consistent modelling of polychromatic ICRH in tokamaks', in Radio-Frequency Power in Plasmas (Proc. 15th Topical Conference on Radio Frequency Power in Plasmas 19-21 May, 2003, Moran, Wyoming, USA), AIP, New York, p. 126-129.
[18]. L.-G. Eriksson, T. Hellsten, and U. Willén, Nucl. Fusion **33** (1993) 1037.
[19]. J. Hedin, T. Hellsten, and J. Carlsson 1998 *Proc. of Joint Varennna-Lausanne Workshop* "*Theory of Fusion Plasmas*" pp. 467, Varenna ISBN 88-7794-167-7"
[20]. J. Hedin, *et al.*, Plasma Phys. Control. Fusion **40** (1998) 1085.
[21]. A. Kaye, *et al*., Fusion Eng. Des. **24** (1994) 1.
[22]. K.G. Budden, Radio Waves in the Ionosphere, Cambridge University Press, Cambridge, 1961.
[23]. A.A. Korotkov, A. Gondhalekar, and A.J. Stuart, Nucl. Fusion **33** (1997) 35.
[24]. D. Testa, *et al*., Plasma Phys. Control. Fusion **46** (2004) S59.

Pulse No:	***B* (T) / I_p (MA)**	**Minority**	**P_{ICRF} (MW)**	**ICRF scheme**	**R_{res} (m) (fraction of power at R_{res})**
56535	3.25 / 1.8	^{3}He	3.5	poly (C+HFS)	2.7 (46%), 2.9 (34%), 3.0 (20%)
56533				poly (C+HFS)	2.7 (55%), 2.9 (23%), 3.0 (22%)
56532				mono (C)	2.9 (46%), 3.0 (24%), 3.05 (30%)
57252	3.7 / 2.0	^{3}He	3.0-3.1	poly (C+LFS)	3.0 (27%), 3.1 (27%), 3.4 (46%),
57245				mono (C)	3.0 (49%), 3.1 (51%)
57300	3.7 / 2.0	^{3}He	4.6	poly (C+LFS)	3.0 (23%), 3.1 (25%), 3.4 (52%)
57301				mono (C)	3.0 (79%), 3.1 (21%)
57296	3.4 / 1.8	H	7.0-7.2	poly (C+LFS)	3.0 (33%), 3.2 (34%), 3.3 (33%)
57298				mono (C)	3.0 (82%), 3.05 (18%)

Table I: Vacuum magnetic field B at R=2.96m, plasma current I_p, minority ion species, total ICRF power P_{ICRF}, ICRF scheme, i.e. monochromatic or polychromatic heating with a central (C), low magnetic-field side (LFS) or high magenetic-field side (HFS) resonance, major radii R_{res} and the applied power fractions of the different resonances. (The magnetic axis is at $R_0 \approx$ 2.95-3m.)

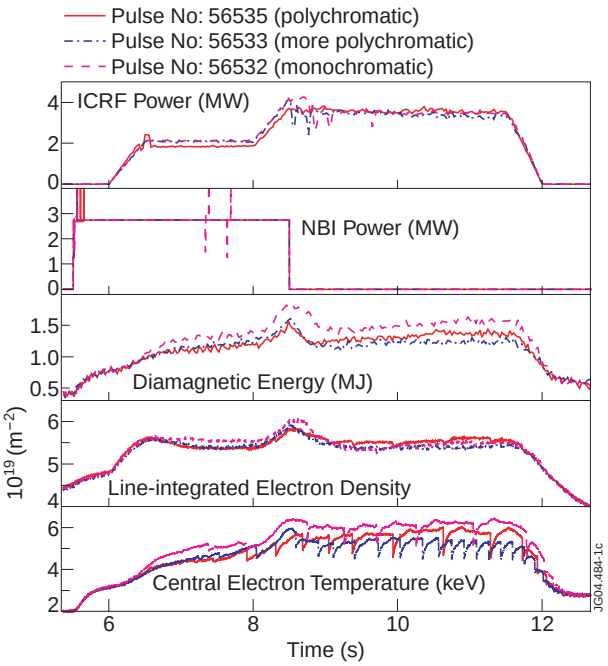

Figure 1: Main plasma parameters for Pulse Nos: 56535, 56533 and 56532 (cf. Table I).

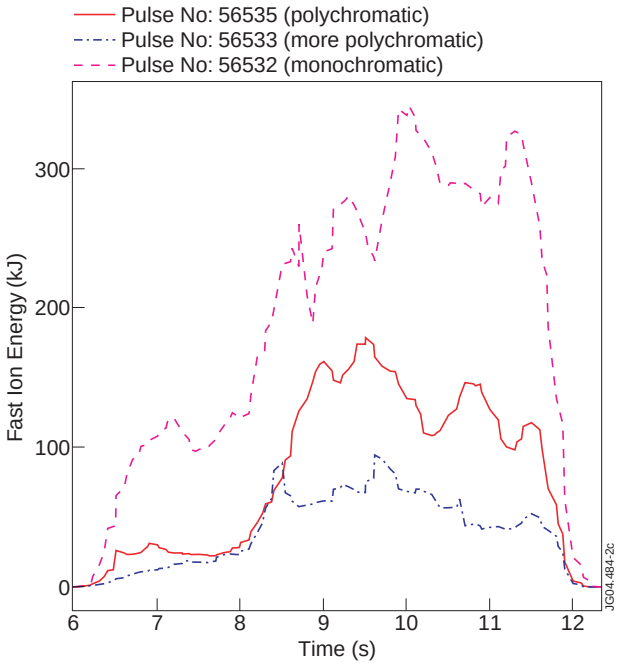

Figure 2: Total fast ion energy W_{fast} as given by the PION code for Pulse Nos: 56535, 56533 and 56532.

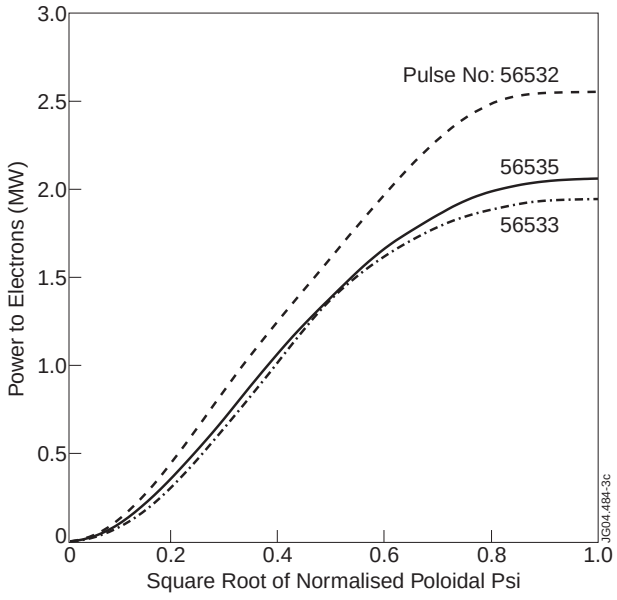

Figure 3: Total electron power deposition profiles as given by the SELFO code for Pulse Nos: 56535, 56533 and 56532.

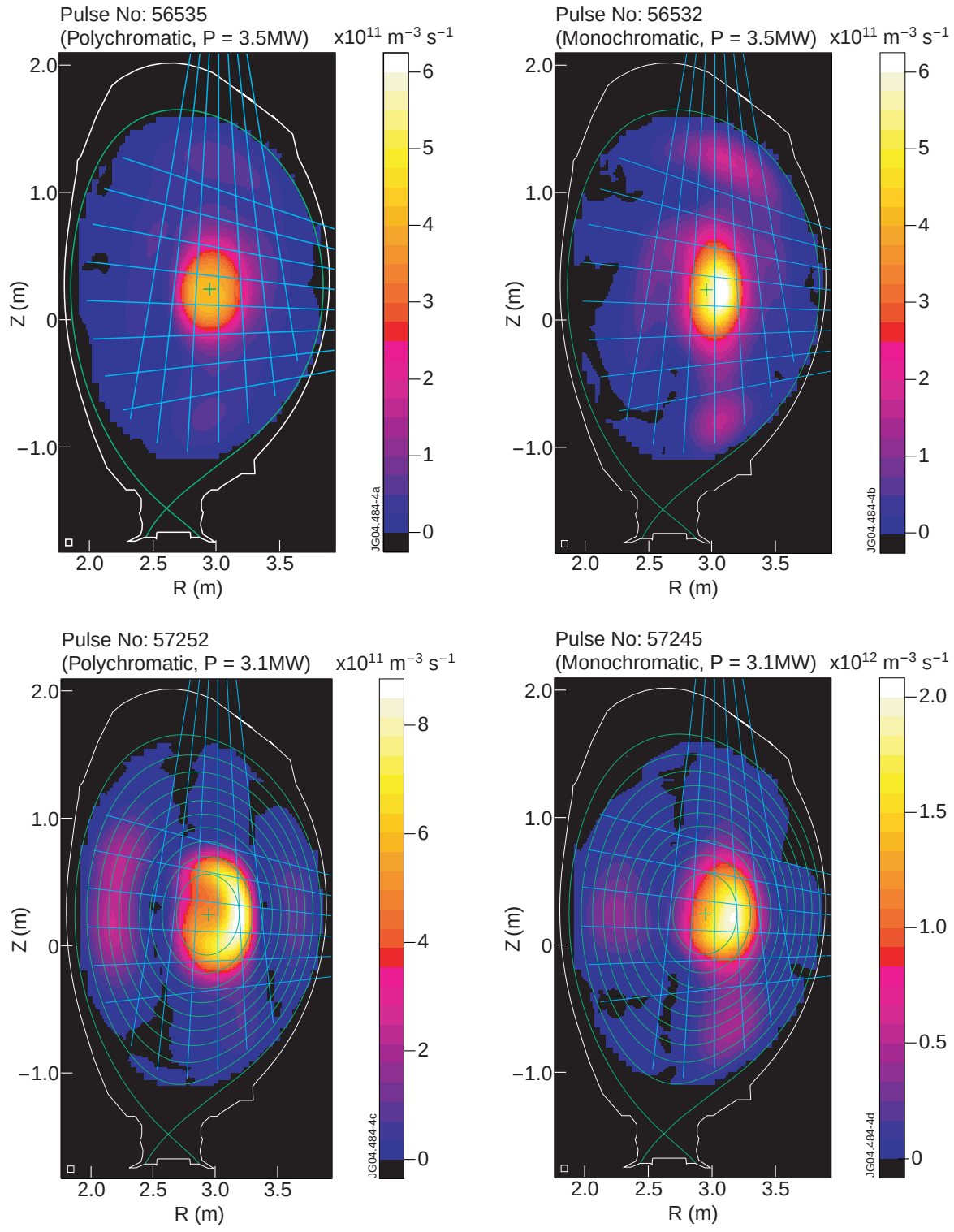

Figure 4: Gamma-ray emissivity in the poloidal plane for (a) Pulse No: 56535, (b) Pulse No: 56532, (c) Pulse No: 57252, (d) Pulse No: 57245,

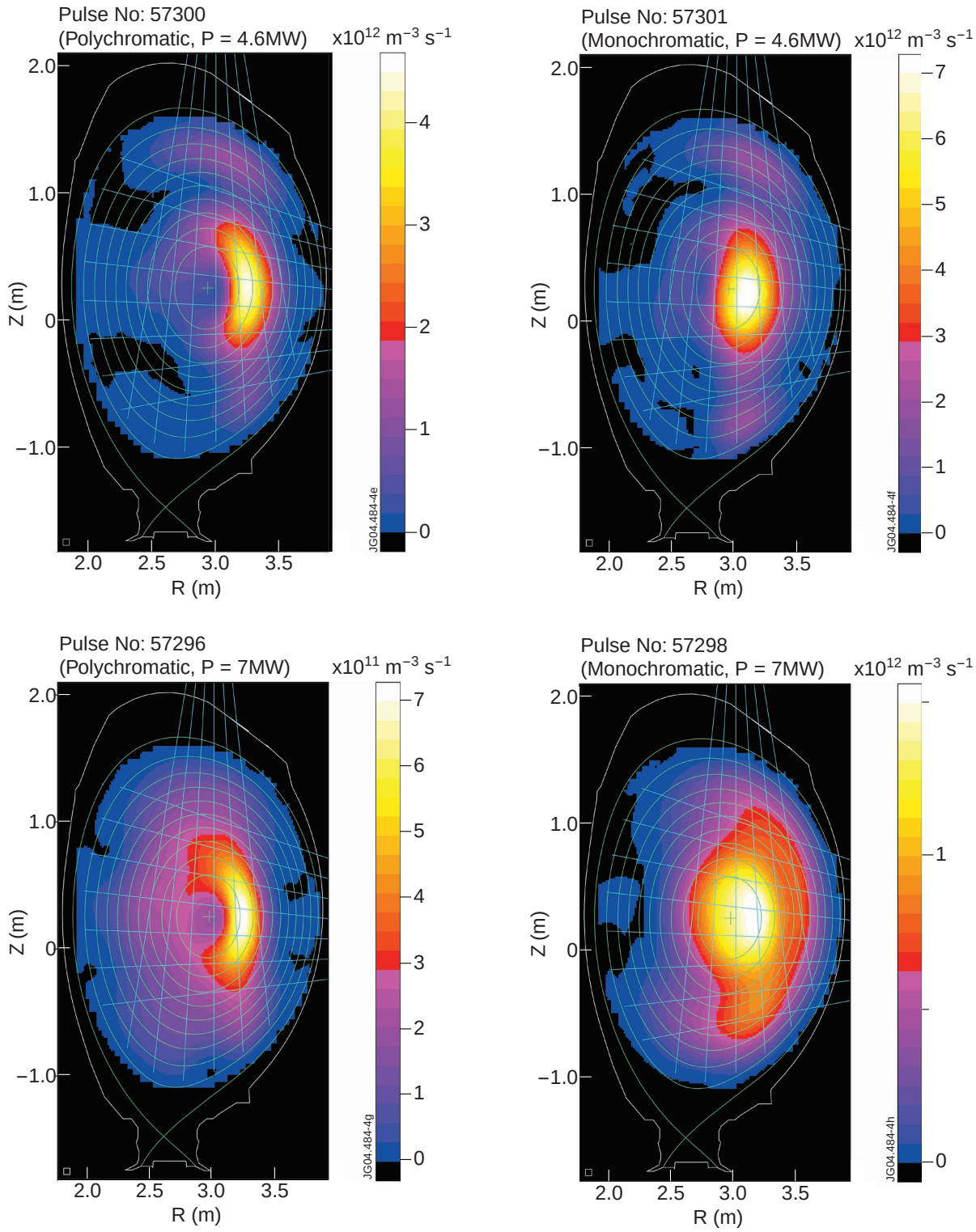

Figure 4: (e) Pulse No: 57300, (f) Pulse No: 57301, (g) Pulse No: 57298 and (h) Pulse No: 57298. The data have been integrated over a one-second time window for all Pulse Nos: except for Pulse No: 57252 where the integral is over two seconds to improve statistics. The lines of sight of the gamma camera [12, 13] are also shown.

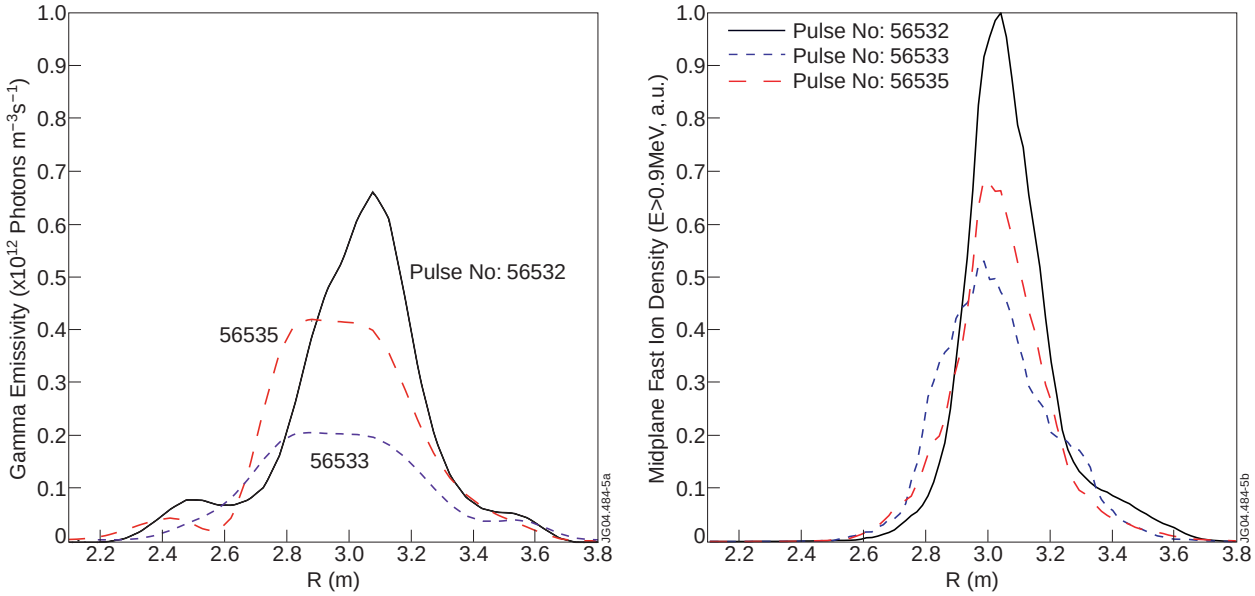

Figure 5: (a) Measured gamma-ray emissivity and (b) distributions of fast ions (E > 0.9MeV) within 0.3m from the midplane as given by the SELFO code for Pulse Nos: 56535, 56533 and 56532. The magnetic axis is at $R_0 \approx 2.95$-3m.

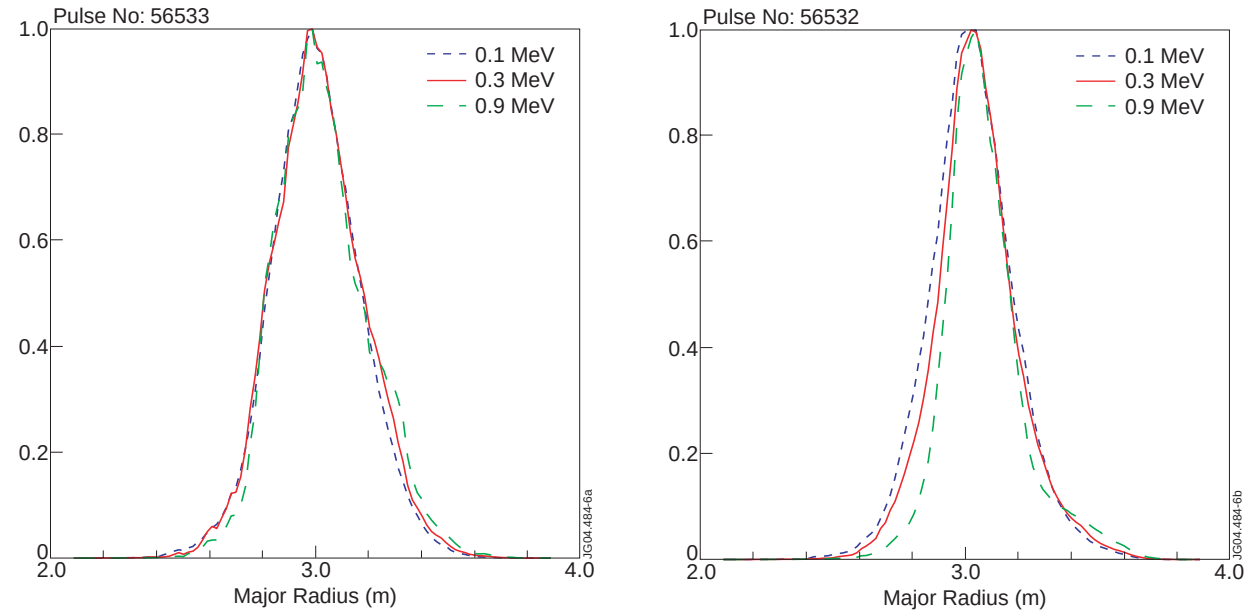

Figure 6: Normalised distributions of fast ions with energies above 0.1, 0.3 and 0.9MeV within 0.3m from the midplane as given by the SELFO code for Pulse Nos: 56533 (polychromatic ICRF) and 56532 (monochromatic ICRF).

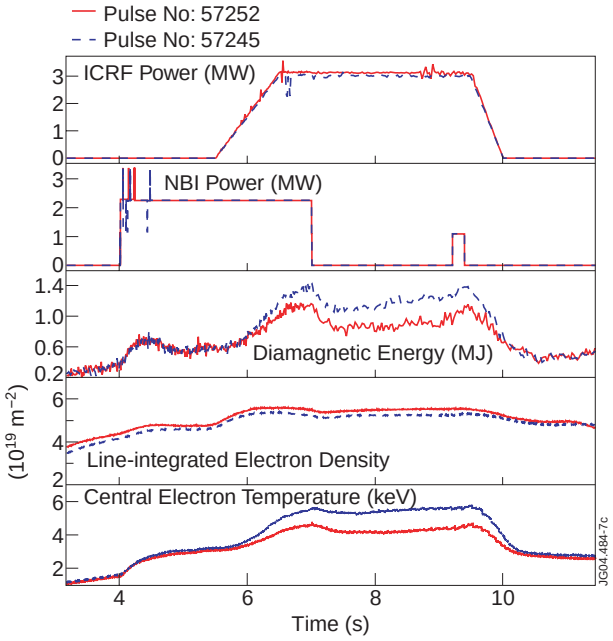

Figure 7: Main plasma parameters for Pulse Nos: 57252 and 57245.

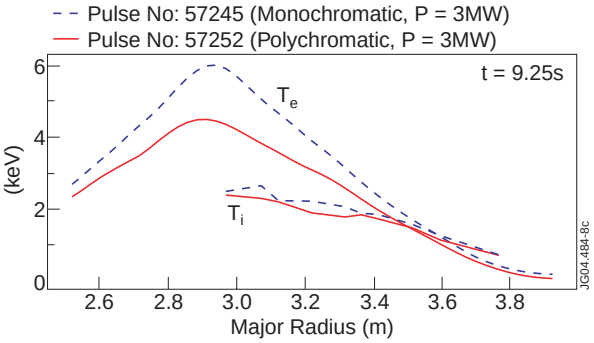

Figure 8: Electron and ion temperature profiles for Pulse Nos: 57252 and 57245.

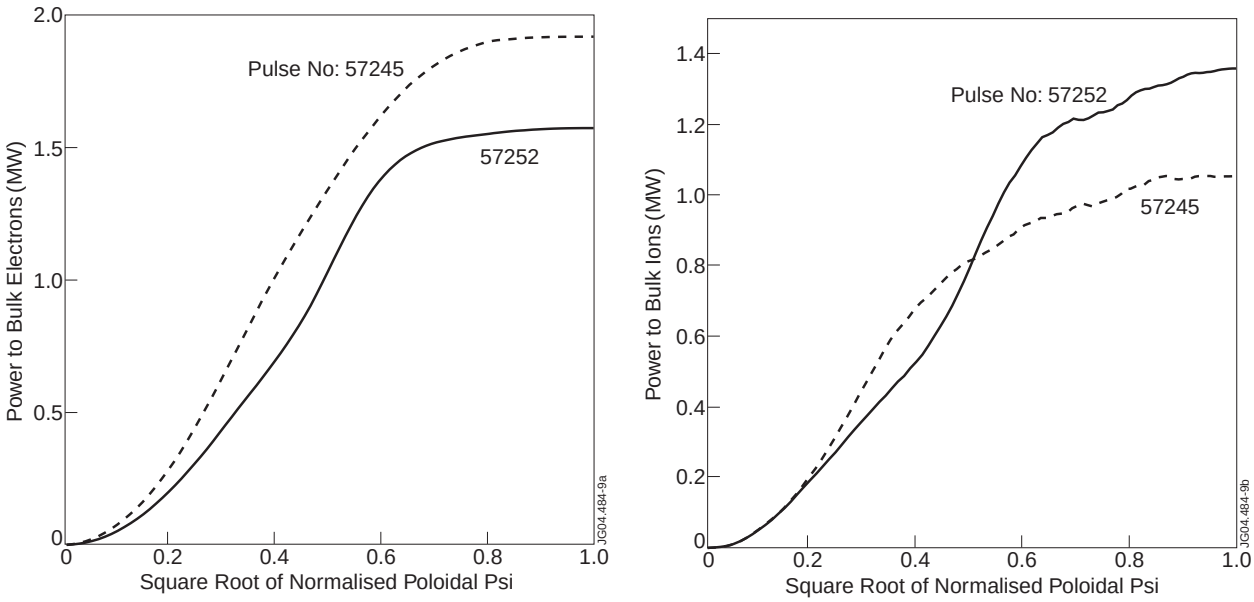

Figure 9: (a) Bulk electron and (b) bulk ion power deposition as given by the SELFO code at t = 8.5s for Pulse Nos: 57252 and 57245.

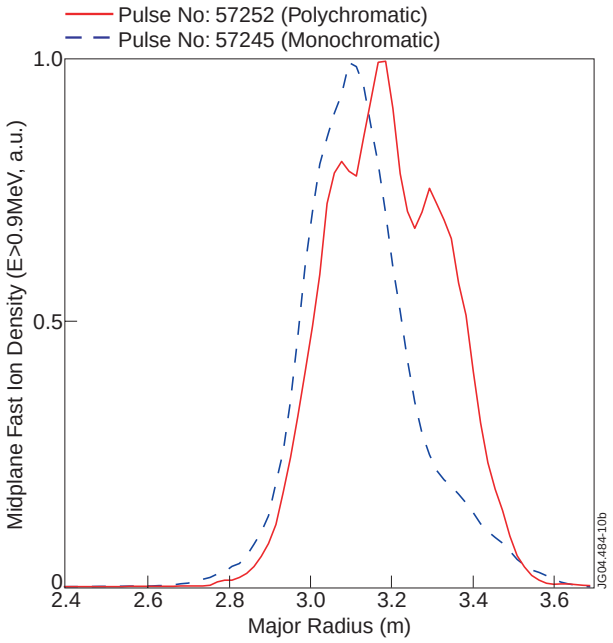

Figure 10: Normalised distributions of fast ions (E > 0.9MeV) within 0.3 m from the midplane as given by the SELFO for Pulse Nos: 57245 and 57252. The magnetic axis is at R_0 = 2.97m.

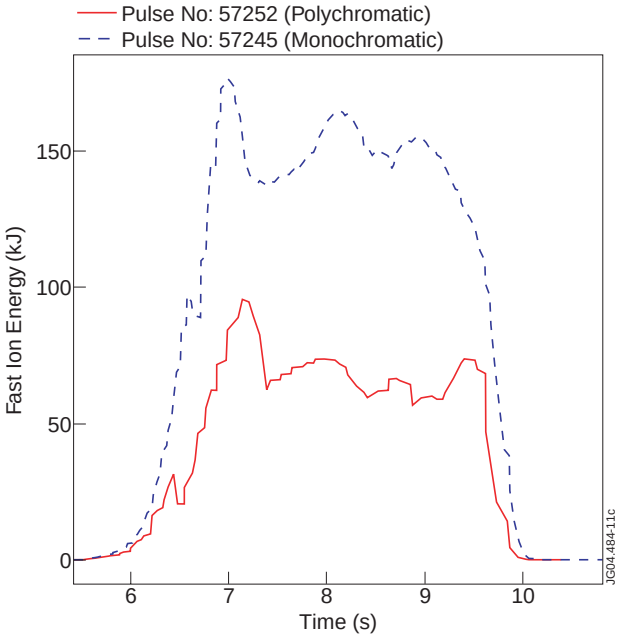

Figure 11: Fast ion energy W_{fast} as given by the PION code for Pulse Nos: 57252 and 57245.

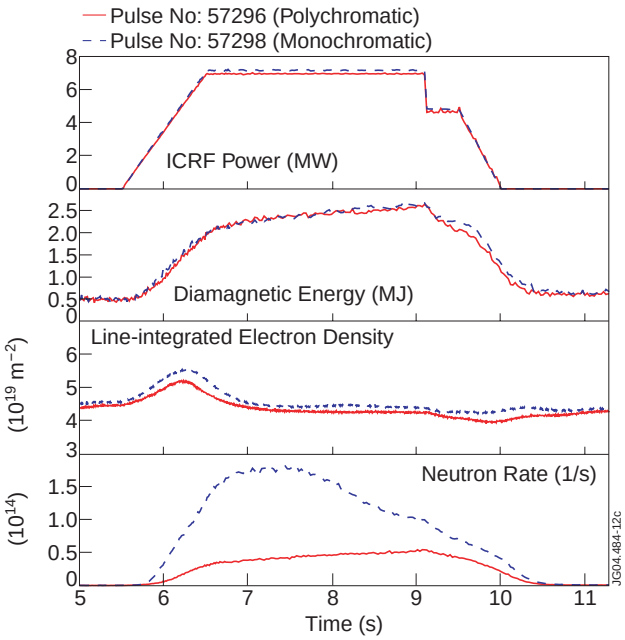

Figure 12: Main plasma parameters for Pulse Nos: 57296 and 57298.